J. exp. Biol. ***180***, *1-13 (1993)*
Printed in Great Britain © The Company of Biologists Limited 1993

THE ULTRASTRUCTURE AND FORMATION OF IRON GRANULES IN THE HONEYBEE (*APIS MELLIFERA*)

CHIN-YUAN HSU and CHIA-WEI LI*

Institute of Life Science, National Tsing Hua University, Hsinchu, Taiwan, R.O.C.

Accepted 25 March 1993

Summary

The honeybee is one of the few organisms that can deposit iron minerals intracellularly. Numerous iron granules are formed in the trophocytes, which are located in the abdomen, beginning on the second day after eclosion. The sequential events of iron deposition in honeybees have been determined and the special features of this biomineralization system are (1) that iron deposition vesicles (IDVs) enlarge by fusing with one another; (2) that dense particles (approx. 7.5nm in diameter) are the basic building blocks in the formation of iron granules; and (3) that a cloudy layer just beneath the membrane of IDVs may play an important role in the formation of the dense particles.

The iron granules seem to be randomly distributed in the trophocytes of the worker and drone. In the queen, however, they are clustered and peripherally located. This distinct difference in the iron granule distribution between members of the hive suggests that these iron granules may have some biological functions. A detailed analysis of total iron content during the life cycle of honeybees has shown that iron granules in the adult worker contain approximately 1% of the total iron content and also account for approximately 3% of the increase in iron content that occurs between the newly eclosed worker stage and the adult worker stage.

Introduction

A variety of organisms, including chitons (Lowenstam, 1962, 1967; Towe and Lowenstam, 1967; Kirschvink and Lowenstam, 1979; Li *et al.* 1989), limpets (Mann *et al.* 1986; St Pierre *et al.* 1986), magnetotactic bacteria (Blakemore, 1975; Frankel *et al.* 1979; Towe and Moench, 1981; Frankel and Blakemore, 1984), honeybees (Kuterbach *et al.* 1982), pigeons (Walcott *et al.* 1979), magnetotactic algae (Torres de Araujo *et al.* 1985) and salmon (Mann *et al.* 1988; Walker *et al.* 1988; Sakaki *et al.* 1990) can deposit iron minerals at ambient temperature, pressure and neutral pH. The structure of these biominerals can be either crystalline or amorphous. Their biological functions are to provide structural support and mechanical strength, to act as iron stores and to play a role in the sensitivity to magnetic or gravitational forces (Mann, 1987; Lowenstam, 1981). The known iron minerals are magnetite (Fe_3O_4), ferrihydrite ($5Fe_2O_3{\cdot}9H_2O$), goethite (α-

*To whom reprint requests should be addressed.

Key words: honeybee, *Apis mellifera*, iron deposition, ultrastructure, development, trophocyte.

FeOOH), lepidocrocite (γ-FeOOH) and amorphous ferric oxides (Mann, 1987). Only magnetotactic bacteria and honeybees are known to be able to deposit iron intracellularly.

Iron minerals are mainly deposited in magnetotactic bacteria as magnetite in magnetosomes, which are arranged in a chain along the motility axis of the cell. The magnetites in magnetosomes can produce permanent magnetic dipole moments and are responsible for magnetotactic responses (Blakemore and Frankel, 1981; Blakemore *et al.* 1981; Frankel and Blakemore, 1989). Iron minerals in honeybees are deposited in a group of specialized cells, the trophocytes, which are situated just beneath the cuticle in the abdomen of adult workers (Kuterbach *et al.* 1982). Iron and minor amounts of phosphorous and calcium are organized into an amorphous structure and are present in membrane-enclosed granules (Kuterbach and Walcott, 1986*a*). These granules, which are randomly distributed in the cytoplasm, are formed in post-eclosion worker bees and increase in both size and number as the worker bees age (Kuterbach and Walcott, 1986*b*).

In this study, the iron content at various developmental stages in the honeybee's life cycle has been analyzed, and the sequential events of iron deposition in worker bees, drones and queen bees have been determined.

Materials and methods

Honeybees, *Apis mellifera*, were bred in an open environment behind the institute building. Sucrose and pollen grains were occasionally added to the hives as dietary supplements. Newly eclosed bees and cells with freshly deposited eggs were marked with colour wash for age identification.

Transmission electron microscopy

Queen bees (about 1 week and 1 year after eclosion), drones (about 1 month after eclosion) and worker bees (just eclosed and 2, 3, 7, 10, 14, 17, 25 and 50 days after eclosion) were freshly collected from the hive and dissected. The ventral abdomens were fixed in 2.5% glutaraldehyde in a $0.1\,\mathrm{mol\,l^{-1}}$ phosphate buffer with $0.35\,\mathrm{mol\,l^{-1}}$ sucrose at pH7.4 and at 25°C for 1.5h, and were postfixed in 1% osmium tetroxide in a $0.1\,\mathrm{mol\,l^{-1}}$ phosphate buffer with $0.35\,\mathrm{mol\,l^{-1}}$ sucrose at pH7.4 for 4h on ice. The postfixed tissues were stained with aqueous saturated uranyl acetate for 20min, dehydrated through an ethanol series and flat-embedded in Spurr's resin. Sections (60–90nm in thickness) were cut with a diamond knife, stained with saturated aqueous uranyl acetate for 30min, followed by Reynold's lead citrate for 3min and then examined in a Hitachi H-600 transmission electron microscope operating at an accelerated voltage of 75kV.

The elemental composition and crystal structure in selected areas of thin sections were analyzed by energy-dispersive X-ray (EDX) microanalysis and by selected-area electron diffraction in a JEOL JEM-2000FX scanning transmission electron microscope operating at an accelerated voltage of 100kV.

Quantitative analysis of iron

The life cycle of the honeybee was divided into thirteen stages (see Table 1). The

newly eclosed worker bees (*N*=17), young worker bees (*N*=30), middle worker bees (*N*=27), adult worker bees (*N*=26) and old worker bees (*N*=20) were dissected and divided into head, thorax, digestive tract, complete abdomen and abdomen without digestive tract. Pollens, honey, royal jelly, intact honeybees (*N*=180) and body parts of worker bees at each development stage were weighed and burned in a porcelain crucible in an oven at 1000˚C for 2h. The ashes were dissolved in $3\,\mathrm{mol\,l^{-1}}$ HCl for 3h, and their iron content was analyzed by using Plamsmakon S-35-induced couple plasma atomic emission spectroscopy.

Isolation of iron granules

Adult worker bees (*N*=1380) were freshly collected from the hive, anaesthetized and thoroughly cleaned using a detergent (Extran), followed by ultrasonication in ice-cold water and extensive rinsing with double-distilled water. Subsequent procedures were carried out at 0–4˚C. The cleaned worker bees were homogenized by using a Polytron homogenizer in $20\,\mathrm{mmol\,l^{-1}}$ Tris–HCl buffer, pH7.6, containing $0.35\,\mathrm{mol\,l^{-1}}$ sucrose and 1% Triton X-100. The homogenate was filtered through a plastic mesh (0.5mm pore size), then centrifuged at $7500\,\boldsymbol{g}$ for 10min. The pellet was resuspended in the above buffer, loaded on sequential sucrose solutions of increasing density, including $1.2\,\mathrm{mol\,l^{-1}}$, $1.6\,\mathrm{mol\,l^{-1}}$, $2.0\,\mathrm{mol\,l^{-1}}$, $2.4\,\mathrm{mol\,l^{-1}}$ and a saturated solution, and centrifuged at $19\,000\,\boldsymbol{g}$ for 1.5h. The resulting pellet was collected, rinsed of all its sucrose using the above buffer and dissolved in $3\,\mathrm{mol\,l^{-1}}$ HCl for 2h. The iron content was analyzed by Plamsmakon S-35-induced couple plasma atomic emission spectroscopy.

Results

Sequential events of iron deposition

In newly eclosed worker bees, the trophocytes are in close association with the epidermal cells but show a tendency to detach from them (Figs 1 and 2). At this stage, the intracellular membrane system of the trophocyte, including the endoplasmic reticulum and Golgi apparatus, are poorly developed, and oil bodies are only partially filled (Fig. 3).

On the second day after eclosion, the endoplasmic reticulum and Golgi apparatus are well defined (Fig. 4), and small vesicles (50–150nm in diameter) containing distinct electron-dense particles (approx. 7.5nm in diameter) can be distinguished by the third day post-eclosion (Figs 5 and 6). These vesicles are destined to be the iron deposition vesicles (IDVs), and the dense particles are the basic building blocks of deposited iron granules.

On the seventh day after eclosion, each IDV has a tightly packed core granule, surrounded by numerous dense particles (Figs 7 and 8) and EDX microanalysis shows that the core granule has a high iron content. A layer of cloudy material is present underneath the membrane of the IDV (Fig. 8), and it seems that the dense particles emerge from this layer and move towards the core granule. Various forms of fusion have been seen between the IDVs, resulting in larger IDVs, transiently containing 2–4 iron core granules (Figs 9 and 10).

On the tenth, fourteenth, and seventeenth days after eclosion, the iron granules continue to grow in size and their ragged surface clearly indicates their relationship with the dense particles (Fig. 11).

On the 25th day after eclosion, the iron granules are mature and average about 0.5±0.1 μm (S.D., *N*=150) in diameter. The cloudy layer disappears, leaving little space between the membrane of the IDV and the iron granule (Fig. 12). Hundreds of iron

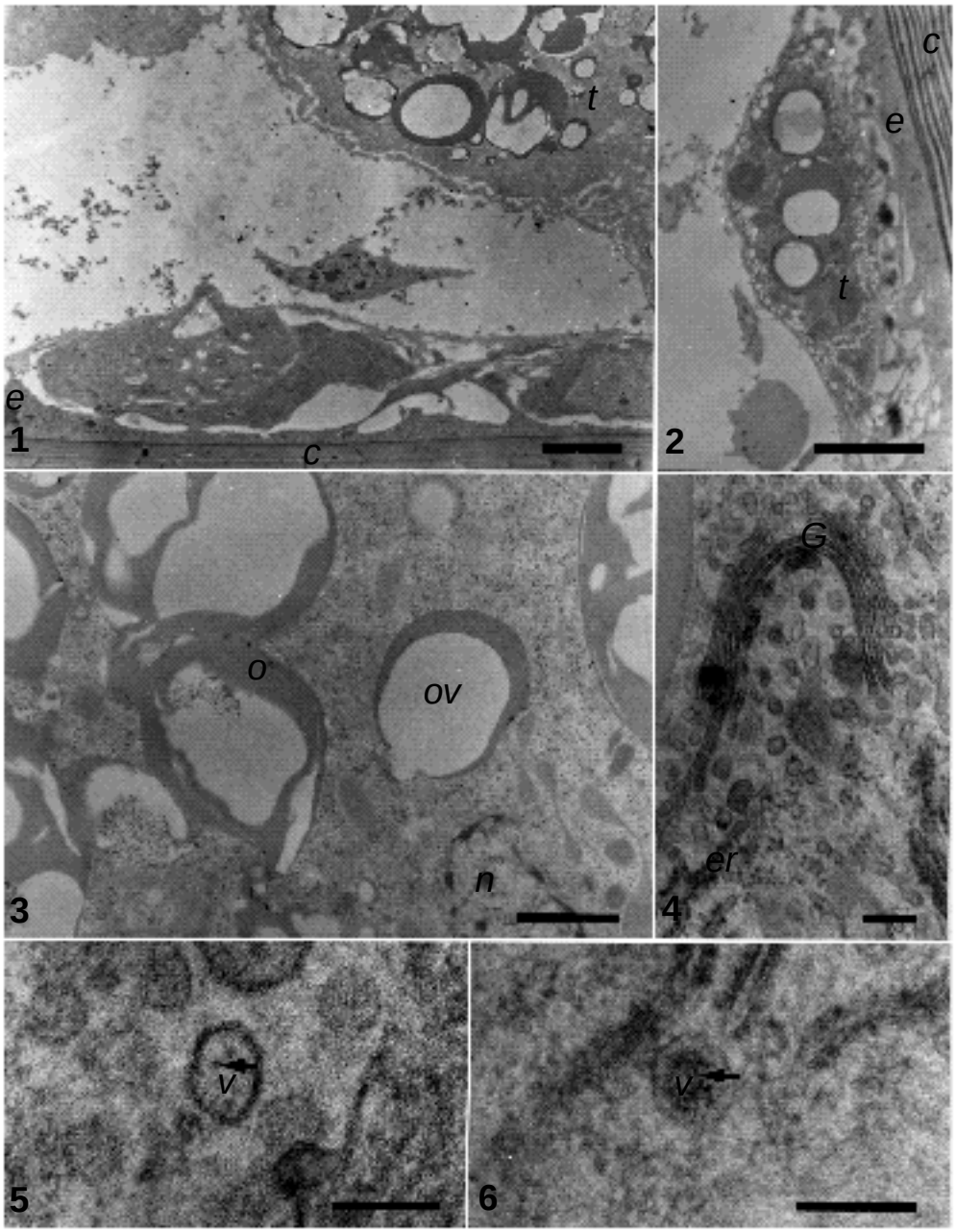

Table 1. *The 13 stages in the life cycle of the honeybee showing the number of days after hatching at which workers, queens and drones enter each stage*

Stage number	Stage name	Number of days after hatching		
		Workers	Queens	Drones
1	Young larva	5	5	5
2	Middle larva	6.5	6.5	6.5
3	Old larva	8	8	8
4	Very young pupa	10	10	11
5	Young pupa	12	11	13
6	Middle pupa	14	12	15
7	Old pupa	16	13	18
8	Very old pupa	19	14	21
9	Newly eclosed	21	16	24
10	Young bee	24–28	18–23	27–31
11	Middle bee	31–39	48–63	37–41
12	Adult bee	46–56	90–100	56–62
13	Old bee	61	200	80

granules have been checked with electron diffraction, and none of them has shown crystalline structures. Some microtubule-like structures have been observed in close proximity to the IDV, with one end attaching to an electron-dense rod on the IDV membrane (Figs 13 and 14).

On the 50th day of eclosion, variations in IDVs were observed. Some IDVs still contained closely packed iron granules, like those seen on the 25th day (see Fig. 12), others contained numerous dense particles and no iron granules, like those seen on the third day after eclosion (see Figs 5 and 6), while others contained irregularly shaped disintegrating iron granules (Fig. 15). At all stages of development, the distribution of iron granules seems to be random within the cell (Fig. 16).

Queen bees and drones also deposited mineral iron in a similar way to the worker bees. Iron granules in the trophocytes of mature drones are randomly distributed (Fig. 17); however, those in mature queen bees are not. In mature queen bees, they are clustered in two or three groups in each cell and are positioned in close proximity to the cell membranes (Figs 18 and 19). Groups of iron granules in neighbouring cells are usually distributed facing each other (Fig. 20).

Figs 1 and 2. Cross sections of the ventral abdomen in the newly eclosed worker bee showing the cuticle (*c*), epidermal cells (*e*) and detaching trophocytes (*t*). Scale bars, 4 μm.

Fig. 3. The intracellular membrane system is poorly developed in the differentiating trophocytes in the worker bee immediately after eclosion and oil vesicles are only partially filled. *o*, oil; *ov*, oil vesicle; *n*, nucleus. Scale bar, 1 μm.

Fig. 4. The endoplasmic reticulum (*er*) and Golgi apparatus (*G*) are well defined in the worker bee on the second day after eclosion. Scale bar, 200nm.

Figs 5 and 6. Vesicles (*v*) with electron-dense particles (arrow) are seen in the worker bee on the third day after eclosion. Scale bar in Fig. 5, 80nm; in Fig. 6, 200nm.

Quantitative analysis of iron content

The total iron content in each worker bee, queen bee and drone has a tendency to increase sharply during the larval stage, maintain a constant level in the pupal stage, and gradually increase through the adult bee stage. For worker bees, the total iron content per individual reaches its highest level (15.7±1.18 μg) (S.D., *N*=180) in middle bees and gradually decreases to 12.2±1.05 μg (S.D., *N*=180) in old bees (Fig. 21).

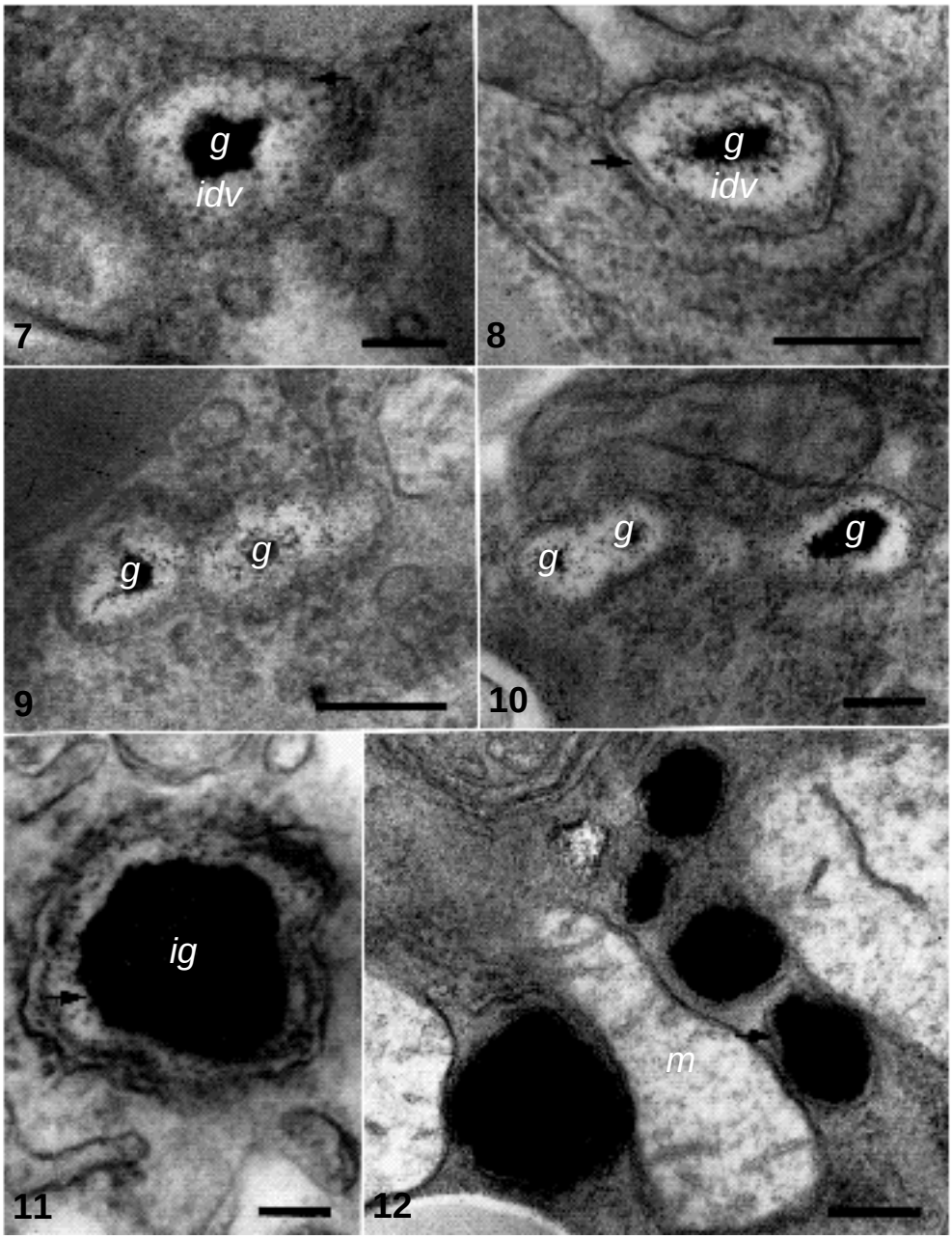

In order to determine the iron content found in the digestive tract, worker bees were dissected and divided into five parts, and the iron content in each part was analysed. Digestive tracts of middle worker bees have the highest iron content (Table 2). The result shows that the iron content of bees measured without the inclusion of the digestive tract also gradually increases from newly eclosed worker bees to adult worker bees and then decreases in old worker bees (Table 2).

Iron in bees should be derived from the diet, which includes pollen, honey and royal jelly. The iron contents of these food sources have been determined to be approximately 0.16 ± 0.02, 0.007 ± 0.001 and $0.13\pm0.01\,\mu g\,mg^{-1}$, respectively.

The iron content of iron granules in an adult worker bee is about $0.13\pm0.01\,\mu g$, that is approximately 1% of the total iron content after deducting the iron content of the digestive tract, and accounts for approximately 3% of the increment in iron content from the newly eclosed worker stage to the adult worker stage.

Discussion

Both honeybees and magnetotactic bacteria deposit iron intracellularly. The special features of iron deposition in the honeybees observed in this study are: (1) that the IDVs fuse with one another to grow into larger ones, (2) that dense particles (approx. 7.5nm in diameter) are the basic building blocks for iron granules, and (3) that a cloudy layer lying beneath the membrane of IDVs may be associated with the formation of dense particles. Apparently this biomineralization system is quite different from that in the magnetotactic bacteria and is also not seen in any extracellular iron deposition systems.

It is well known that magnetite crystals within bacterial magnetosomes are single magnetic domains (Frankel and Blakemore, 1984) and their size varies greatly with species, between approximately 50 and 300nm (Vali and Kirschvink, 1990). No subunits were observed in the formation of bacterial magnetite and no visible organic matrix was present in the magnetosomes (Gorby *et al.* 1988). We are uncertain about the origin of the primary IDVs, although they usually occurred in the vicinity of the abundant endoplasmic reticulum. The origin of the bacterial magnetosome membranes is also a mystery: they do not appear to be contiguous with the cytoplasmic membrane and have some unique protein components (Gorby *et al.* 1988).

Figs 7 and 8. In the iron deposition vesicle (*idv*), aggregation of the dense particles forms a core granule (*g*) in the worker bee on the seventh day after eclosion. A layer of cloudy material (arrow) is present underneath the membrane of the iron deposition vesicle. Scale bar in Fig. 7, 80nm; in Fig. 8, 200nm.

Fig. 9. Fusion of two IDVs in the worker bee on the seventh day after eclosion. *g*, granule. Scale bar, 200nm.

Fig. 10. Fusion of three IDVs in the worker bee on the seventh day after eclosion. *g*, granule. Scale bar, 200nm.

Fig. 11. Detail of an IDV in the worker bee on the tenth day after eclosion, showing the iron granule (*ig*) with a ragged surface (arrow). Scale bar, 80nm.

Fig. 12. Most of the IDVs in the worker bee on the 25th day after eclosion are mature, with little space (arrow) left between the membrane and the iron granule. *m*, mitochondria. Scale bar, 200nm.

No electron-dense materials containing iron, e.g. ferritin aggregates, were found outside the IDVs. Iron must be transported into the IDV by carriers on the IDV membrane, although the cytoplasmic form of iron is unknown. This process has also been suggested in magnetotactic bacteria (Frankel and Blakemore, 1984; Vali and Kirschvink, 1990). The membrane of the IDVs in honeybees is about 8nm thick and consists of a lipid bilayer, whereas that of the bacterial magnetosome is about 5.6nm thick. Proteins that only occur in the magnetosomal membrane and that may be related to iron deposition have been purified (Gorby *et al.* 1988). We are currently isolating membrane proteins from the IDVs of honeybees.

Providing bees with a diet deficient in iron might provide important clues to the iron

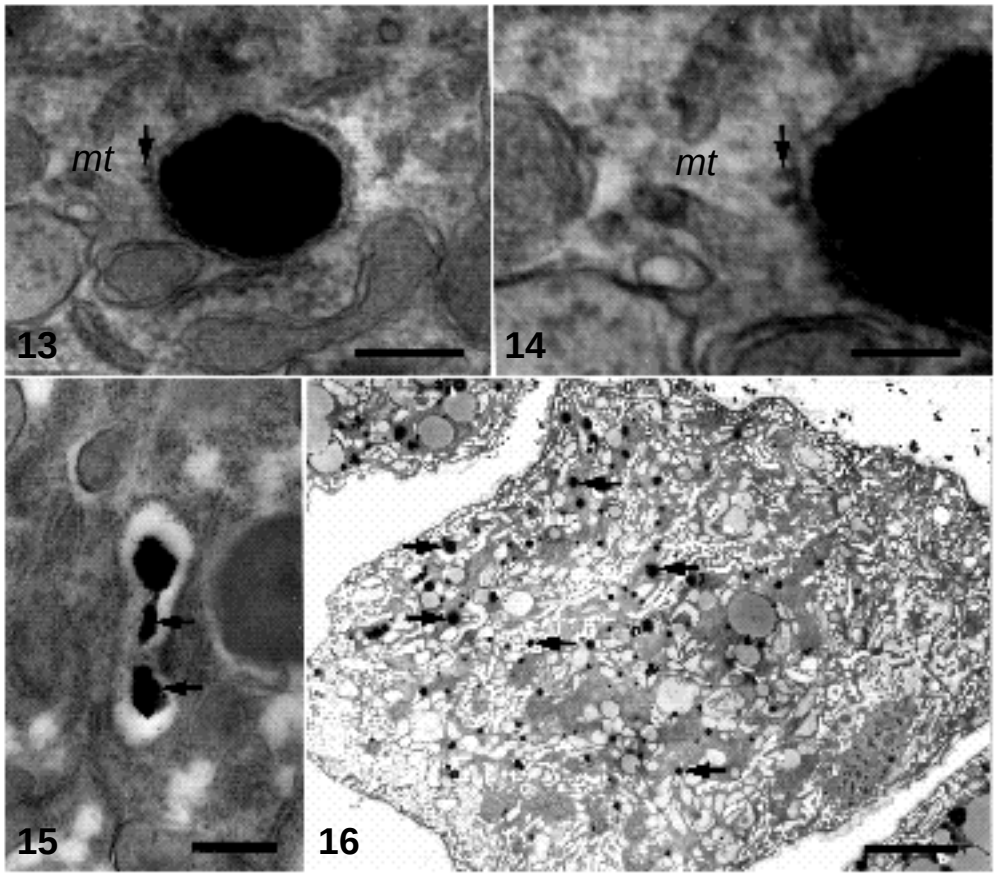

Figs 13 and 14. Regularly spaced microtubule-like structures (*mt*) were observed in close proximity to the IDV, with one end attached to an electron-dense rod (arrow) on the IDV membrane in the worker bee on the 25th day after eclosion. Scale bar in Fig. 13, 200nm; in Fig. 14, 100nm.

Fig. 15. Iron granules in some of the IDVs in the worker bee on the 50th day after eclosion show signs of disintegration (arrows). Scale bar, 400nm.

Fig. 16. Iron granules (arrows) appear to be randomly distributed within the trophocyte of the worker bee. Scale bar, 4μm.

deposition process, but it is extremely difficult to maintain bees on an iron-free diet, since pollen, high in iron content in nature, is the essential food for bees and there is no suitable substitute. An experiment carried out on magnetotactic bacteria cultured in the absence of

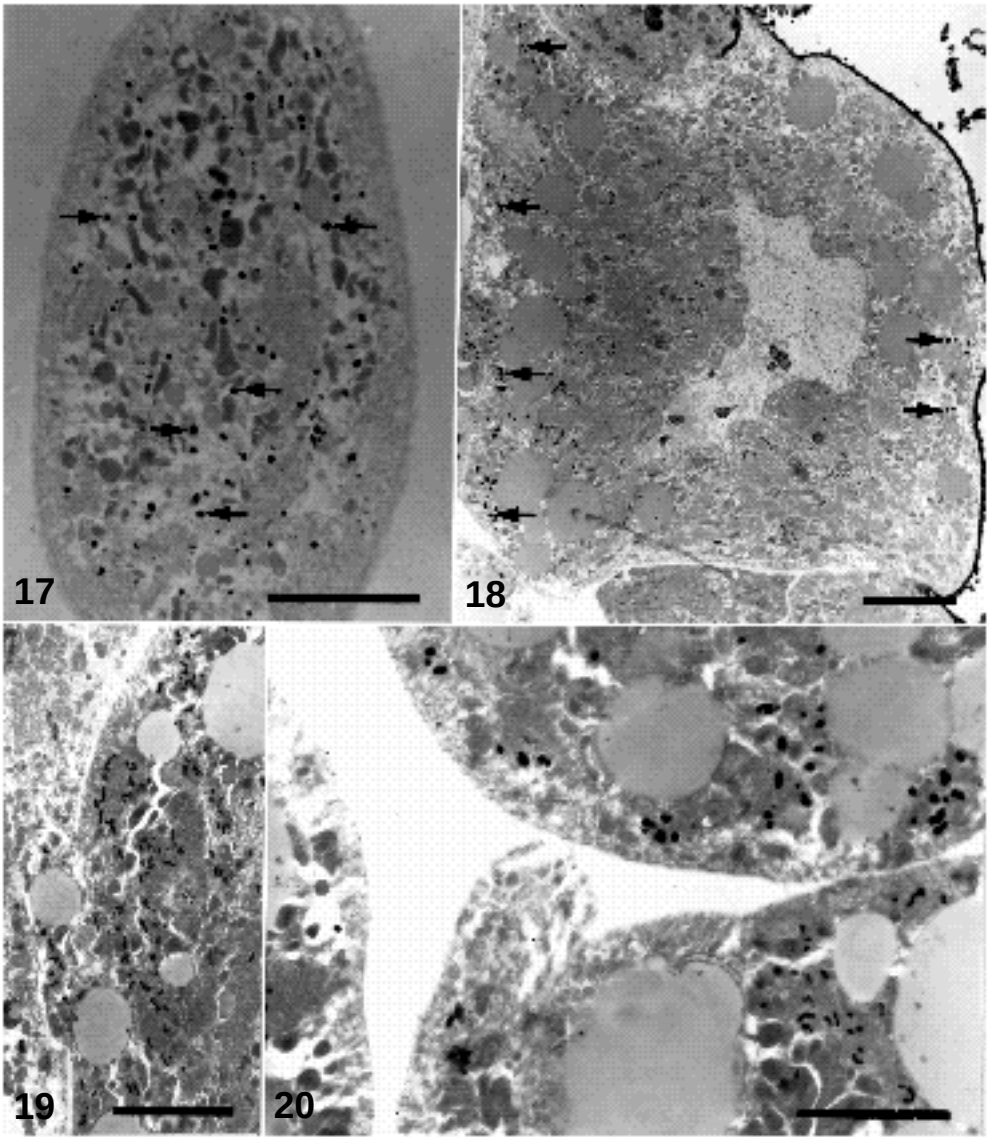

Fig. 17. The iron granules (arrows) are distributed randomly in the drone trophocyte. Scale bar, 4 μm.

Figs 18 and 19. In the queen bee, the iron granules are clustered in two or three groups (arrows) in each cell and are positioned in close proximity to the cell membrane. Scale bar in Fig. 18, 8 μm; in Fig. 19, 4 μm.

Fig. 20. Groups of iron granules in neighbouring cells in the queen bee are distributed facing each other. Scale bar, 4 μm.

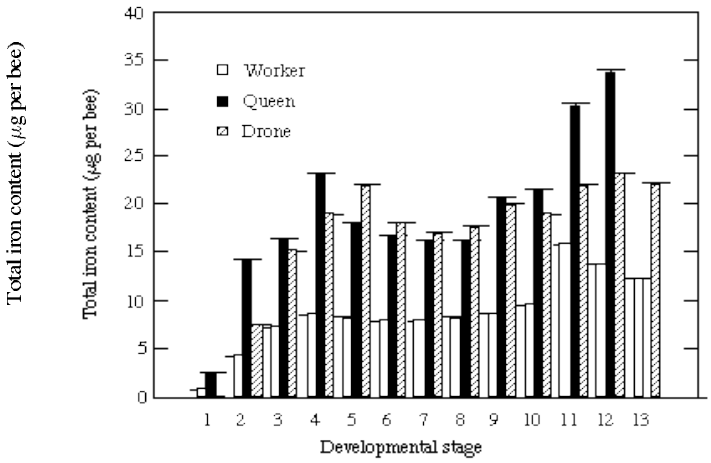

Fig. 21. The total iron content in each worker bee, queen bee and drone at different developmental stages. Values are mean ± S.D., *N*=180 workers; *N*=10 queens; *N*=30 drones.

iron showed that some empty magnetosomes were present in the cells (Gorby *et al.* 1988). This might imply that vesicle formation and iron deposition are, at least in part, independent events, i.e. it is not the presence of excess iron in the cell that triggers the formation of magnetosome vesicles.

The cloudy layer, visualized by uranyl acetate and lead citrate staining, is probably organic in nature and we suggest that it is the likely site at which all intermediate iron conversion processes occur, i.e. imported iron is deposited into dense particles in this region. Iron granules in the IDVs apparently arise from the aggregation of numerous dense particles. However, at this stage there is no evidence to determine whether it is a self-assembling or a matrix-mediated process.

Worker bees fly and forage for food during daylight. Their iron granules are distributed randomly in the trophocyte. Queen bees reside in the hive for most of their life. Their iron granules are clustered and positioned in close proximity to the cell membranes. The differential distribution between the two castes suggests that the iron granules have some biological functions. The increase in iron content from the newly eclosed worker stage to the adult worker stage, where only 3% was due to deposited iron granules, suggests that iron granules may have little to do with the excretion of waste, with iron storage or with iron homeostasis. The iron granules again appear to have some biological functions which may be related to the bees' orientation. It has been suggested that the orientation of honeybees may be affected by the earth's magnetic field, and it has been demonstrated that directional information conveyed by the waggle dance and nest-building can be influenced by the geomagnetic field (Lindauer and Martin, 1968). Studies have also detected magnetic remanence in the front of the abdomen of worker bees (Gould *et al.* 1978). Numerous iron granules found in the trophocyte of the abdomen are thought to

Table 2. *The iron content of head, thorax, abdomen, abdomen without digestive tract and digestive tract per worker bee in the different developmental stages*

	Iron content (μg per bee)					
Stages	Total*	Head†	Thorax†	Complete abdomen†	Abdomen without digestive tract†	Digestive tract†
Eclosed worker bee	8.56±1.34	1.60±0.52 (17)	3.06±0.81 (17)	3.76±0.47 (17)	2.36±0.41 (17)	1.45±0.32 (17)
Young worker bee	9.55±1.73	1.45±0.43 (30)	2.51±0.75 (30)	6.47±0.59 (30)	3.61±0.38 (30)	2.12±0.36 (30)
Middle worker bee	15.7±1.18	1.11±0.58 (27)	4.39±0.68 (27)	9.91±0.68 (27)	4.34±0.42 (27)	5.43±0.44 (27)
Adult worker bee	13.6±1.47	1.43±0.37 (26)	5.08±0.78 (26)	7.08±0.56 (26)	4.91±0.46 (26)	2.19±0.37 (26)
Old worker bee	12.2±1.05	0.99±0.61 (20)	4.95±0.63 (20)	6.08±0.54 (20)	4.51±0.36 (20)	1.58±0.32 (20)

*Values are mean ± S.D., N=180.
†Data are expressed as mean ± S.D., (N).

contain small amounts of magnetite (Kuterbach *et al.* 1982). Honeybees have also been trained to distinguish magnetic fields of varying intensities (Walker and Bitterman, 1985). It has also been suggested that, although honeybees can sense weak magnetic fields, they do not use this information as a directional cue (Tenforde, 1989). It can be concluded that honeybees can sense magnetic fields, although the relationship between iron granules and magnetoreception is unknown.

The random distribution and amorphous nature of iron granules (Kuterbach *et al.* 1982; Kuterbach and Walcott, 1986*b*) makes them useless for magnetoreception unless the cytoskeleton anchors the IDVs to the cell membrane. It has previously been reported that the cell linings between trophocytes have many gap junctions, allowing the rapid transmission of electrical and chemical signals between coupled cells, although neuroanatomical studies have revealed that the trophocytes are not innervated (Kuterbach and Walcott, 1986*a*). Regularly spaced microtubule-like structures have been observed to be positioned in close proximity to the IDVs of worker bees. It is not known how firm the association is, but movement of the granule might induce the cytoskeleton to trigger the transduction mechanism. The signals might then be magnified *via* the gap junctions. The mechanism of magnetoreception in honeybees may be similar to that of gravitropism in plant roots (Wendt *et al.* 1987; Sievers *et al.* 1989), where microfilaments are physically associated with statoliths and are probably involved in the gravitropic response. Since the fixation of material from drones and queen bees was not as good as that from worker bees in this study, we were unable to determine whether microtubule-like structures were also associated with the IDVs in these castes.

The reason for the disintegration of the iron granules at the old worker stage is not known. This phenomenon has not been observed in other iron deposition systems and more work is needed to clarify this point.

This study was supported by grants NSC 80–0203-B007–14 and NSC 81–0203-B007–507 from the National Science Council, ROC.

References

BLAKEMORE, R. P. (1975). Magnetotactic bacteria. *Science* **190**, 377–379.

BLAKEMORE, R. P. AND FRANKEL, R. B. (1981). Magnetic navigation in bacteria. *Scient. Am.* **245**, 58–65.

BLAKEMORE, R. P., FRANKEL, R. B. AND KALMIJN, A. J. (1981). Southseeking magnetotactic bacteria in the southern hemisphere. *Nature* **286**, 384–385.

FRANKEL, R. B. AND BLAKEMORE, R. P. (1984). Precipitation of Fe_3O_4 in magnetotactic bacteria. *Phil. Trans. R. Soc. Lond. B* **304**, 567–574.

FRANKEL, R. B. AND BLAKEMORE, R. P. (1989). Magnetite and magnetotaxis in microorganisms. *Bioelectromagnetics* **10**, 223–237.

FRANKEL, R. B., BLAKEMORE, R. P. AND WOLFE, R. S. (1979). Magnetite in freshwater magnetotactic bacteria. *Science* **203**, 1355–1356.

GORBY, Y. A., BEVERIDGE, T. J. AND BLAKEMORE, R. P. (1988). Characterization of the bacterial magnetosome membrane. *J. Bacteriol.* **170**, 834–841.

GOULD, J. L., KIRSCHVINK, J. L. AND DEFFEYES, K. S. (1978). Bees have magnetic remanence. *Science* **201**, 1026–1028.

KIRSCHVINK, J. L. AND LOWENSTAM, H. A. (1979). Mineralization and magnetization of chiton teeth: paleomagnetic, sedimentologic and biologic implications of organic magnetite. *Earth Planet. Sci. Lett*. **44**, 193–204.

KUTERBACH, D. A. AND WALCOTT, B. (1986*a*). Iron-containing cells in the honey-bee (*Apis mellifera*). I. Adult morphology and physiology. *J. exp. Biol.* **126**, 375–387.

KUTERBACH, D. A. AND WALCOTT, B. (1986*b*). Iron-containing cells in the honey-bee (*Apis mellifera*). II. Accumulation during development. *J. exp. Biol.* **126**, 389–401.

KUTERBACH, D. A., WALCOTT, B. R., REEDER, J. AND FRANKEL, R. B.(1982). Iron-containing cells in the honey bee (*Apis mellifera*). *Science* **218**, 695–697.

LI, C. W., CHIN, T. S., LI, J. S. AND HUANG, S. H. (1989). Growth of chiton teeth evidenced from magnetic measurment and microstructure characterization. *IEEE Trans. Magnet.* **25**, 3818–3820.

LINDAUER, M. AND MARTIN, H. (1968). Die Schwereorientierung der Bienen unter dem Einfluss des Erdmagnetfeldes. *Vergl. Physiol.* **60**, 219–243.

LOWENSTAM, H. A.(1962). Magnetite in denticle capping in recent chitons (*Polyplacophora*). *Geol. Soc. Am. Bull.* **73**, 435–438.

LOWENSTAM, H. A. (1967). Lepidocrocite, an apatite mineral and magnetite in teeth of chitons (Polyplacophora). **156**, 1373–1375.

LOWENSTAM, H. A.(1981). Minerals formed by organisms. *Science* **211**, 1126–1131.

MANN, S. (1987). Biomineralization of iron oxides. *Chem. Britain* **23**, 137–140.

MANN, S., PERRY, C. C., WEBB, J., LUKE, B. AND WILLIAMS, R. J. P. (1986). Structure, morphology, composition and organization of biogenic minerals in limpet teeth. *Proc. R. Soc. Lond. B* **227**, 179–190.

MANN, S., SPARKS, N. H. C., WALKER, M. M. AND KIRSCHVINK, J. L.(1988). Ultrastructure, morphology and organization of biogenic magnetite from sockeye salmon, *Oncorhynchus nerka*: implications for magnetoreception. *J. exp. Biol.* **126**, 375–387.

SAKAKI, Y., MOTOMIYA, T., KATO, M. AND OGURA, M.(1990). Possible mechanism of biomagnetic sense organ extracted from sockeye salmon. *IEEE. Trans. Magnet.* **26**, 1554–1556.

SIEVERS, A., KRUSE, S., KUO-HUANG, L.-L. AND WENDT, M. (1989). Statoliths and microfilaments in plant cells. *Planta* **172**, 321–329.

ST PIERRE, T. G., MANN, S., WEBB, J., DICKSON, D. P. E., RUNHAM, N. W. AND WILLIAMS, R. J. P.(1986). Iron oxide biomineralization in the radula teeth of the limpet *Patella vulgata*: Mossbauer spectroscopy and high resolution transmission electron microscopy studies. *Proc. R. Soc. Lond. B* **228**, 31–42.

TENFORDE, T. S. (1989). Electroreception and magnetoreception in simple and complex organisms. *Bioelectromagnetics* **10**, 215–221.

TORRES DE ARAUJO, F. F., PIRES, M. A., FRANKEL, R. B. AND BICUDO, C. E. M. (1985). Magnetite and magnetotaxis in algae. *Biophys. J.* **50**, 375–378.

TOWE, K. M. AND LOWENSTAM, H. A. (1967). Ultrastructure and development of iron mineralization in the radular teeth of *Cryptochiton stelleri* (mollusca). *J. Ultrastruct. Res.* **17**, 1–13.

TOWE, K. M. AND MOENCH, T. T. (1981). Electron-optical characterization of bacterial magnetite. *Earth Planet. Sci. Lett.* **52**, 213–220.

VALI, H. AND KIRSCHVINK, J. L. (1990). Observations of magnetosome organization, surface structure and iron biomineralization of undescribed magnetic bacteria: evolutionary speculations. In *Iron Biominerals* (ed. R. B. Frankel and R. P. Blakemore), pp. 97–115. Plenum Press: New York.

WALCOTT, C., GOULD, J. L. AND KIRSCHVINK, J. L. (1979). Pigeons have magnetites. *Science* **205**, 1027–1029.

WALKER, M. M. AND BITTERMAN, M. E. (1985). Conditioned responding to magnetic fields by honeybees. *J. comp. Physiol.* A**157**, 67–71.

WALKER, M. M., QUINN, T. P., KIRSCHVINK, J. L. AND GROOT, C. (1988). Production of single-domain magnetite throughout life by sockeye salmon, *Oncorhynchus nerka. J. exp. Biol.* **126**, 375–387.

WENDT, M., KUO-HUANG, L.-L. AND SIEVERS, A. (1987). Gavitropic bending of cress roots without contact between amyloplasts and complexes of endoplasmic reticulum. *Planta* **172**, 321–329.